ISTITUTO NAZIONALE DI FISICA NUCLEARE
Laboratori Nazionali di Frascati

LNF-80/23

B. Esposito et al.:
INCLUSIVE STUDY OF HADRON PRODUCTION BY e^+e^- ANNIHILATION FOR $1.4 \leq \sqrt{s} \leq 2.3$ GeV AT ADONE.

Estratto da:
Nuovo Cimento 55A, 437 (1980)

Servizio Documentazione
dei Laboratori Nazionali di Frascati
Cas. Postale 13 - Frascati (Roma)

IL NUOVO CIMENTO Vol. 55 A, N. 4 21 Febbraio 1980

Inclusive Study of Hadron Production by e^+e^- Annihilation for $1.4 \leqslant \sqrt{s} \leqslant 2.3$ GeV at Adone.

B. Esposito, F. Felicetti (*), A. Marini, G. Piano Mortari and F. Ronga

Istituto Nazionale di Fisica Nucleare - Sezione di Frascati, Italia
Laboratori Nazionali di Frascati - Frascati, Italia

D. Bisello, M. Nigro and L. Pescara

Istituto di Fisica dell'Università - Padova, Italia
Istituto Nazionale di Fisica Nucleare - Sezione di Padova, Italia

R. Bernabei, S. d'Angelo, P. Monacelli, M. Moricca, L. Paoluzi
R. Santonico and F. Sebastiani

Istituto di Fisica dell'Università - Roma, Italia
Istituto Nazionale di Fisica Nucleare - Sezione di Roma, Italia

(ricevuto il 22 Giugno 1979)

Summary. — Results are reported on the inclusive study of the production of charged particles in the reaction $e^+e^- \to$ many hadrons in the c.m. energy range $\sqrt{s} = (1.4 \div 2.3)$ GeV. The ratio between the kaons detected in the MEA apparatus at Adone and the corresponding total number of particles has been measured. The inclusive momentum distributions of the detected particles are given and the mean charged-particle energy and the mean observed multiplicity are evaluated.

1. – Introduction.

Results are reported on the inclusive study of the production of charged particles in the reaction

(1) $$e^+ + e^- \to \text{many hadrons}$$

(*) Present address: Comitato Nazionale per l'Energia Nucleare, Roma.

in the centre-of-mass energy range $\sqrt{s} = (1.4 \div 2.3)$ GeV, by using the magnetic detector MEA at Adone.

The MEA apparatus, described in detail in ref. [1], consists (fig. 1) of a solenoidal magnet transverse to the e^+e^- intersection region and of a set of

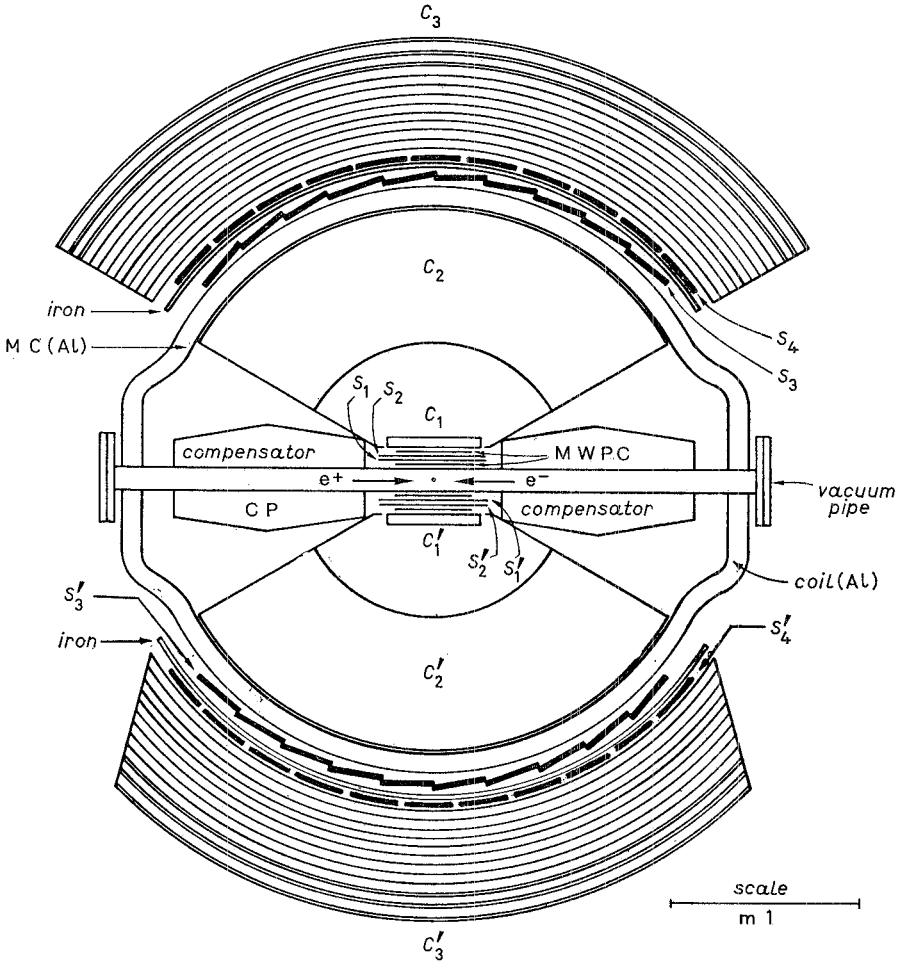

Fig. 1. – Vertical section of the experimental apparatus: C_1, C_1' are narrow-gap spark chambers; C_2, C_2' wide-gap cylindrical spark chambers for momentum analysis; C_3, C_3' thick-plate spark chambers for particle identification; MWPC multiwire proportional chambers; S_1, S_2, ..., S_4' scintillation counters.

---

[1] W. W. Ash, D. C. Cheng, B. Esposito, F. Felicetti, A. Marini, H. Ogren, I. Peruzzi, M. Piccolo, F. Ronga, G. Sacerdoti, L. Trasatti, G. T. Zorn, B. Bartoli, B. Coluzzi, A. Nigro, V. Silvestrini, F. Vanoli, D. Bisello, A. Mulachié, M. Nigro, L. Pescara, R. Santangelo, E. Schiavuta, D. Scannicchio, P. Monacelli, L. Paoluzi, G. Piano Mortari and F. Sebastiani: *Nucl. Instrum. Methods*, **148**, 431 (1978).

optical spark chambers, multiwire proportional chambers and scintillation counters. The trigger requires at least two charged particles with a minimum kinetic energy of 130 MeV (if pions), in the two opposite halves of the apparatus. Events from reaction (1) are required to present *a*) two nonshowering charged particles observed with an acoplanarity angle $\Delta\varphi \geqslant 10°$, or more than two charged particles detected; *b*) correct timing with respect to the bunch-bunch collisions; *c*) proper position of the source points as measured by the multiwire proportional chambers.

The spark chamber tracks, recorded on film, have been measured with « mangiaspago » for the determination of the direction and momentum of the detected particles.

2. – Measurement of the kaon fraction.

The ratio between the kaons detected by the apparatus and the corresponding total number of particles has been measured.

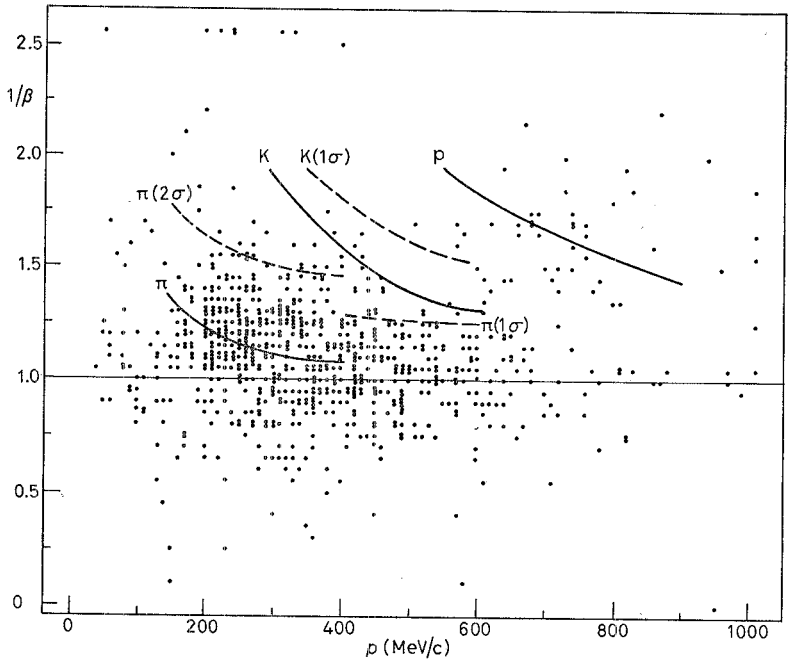

Fig. 2. – Scatter plot of $1/\beta$ *vs.* p for all particles which satisfy the selection criteria, both positive and negative. Full lines correspond to particles with pion, kaon or proton masses and dashed lines are obtained by displacing the previous ones by one or two standard deviations in time of flight.

The momentum range in which it is possible to distinguish between pions and kaons through momentum *vs.* time-of-flight measurements is (400 ÷ 600) MeV/c for the MEA apparatus.

Time of flight was measured on a mean basis of 1 m between counters S_1, S_2 and S_1', S_2' placed directly above and below the interaction region and each of the twenty counters S_3 and S_3' placed just behind the coil of the magnet.

The lower-momentum cut (400 MeV/c) is essentially due to the thickness of the coil. The value of the β of the single particle was obtained from the time-of-flight measurement, corrected by the pulse height of the counters and by taking into account the effective length of the particle trajectory between the counters.

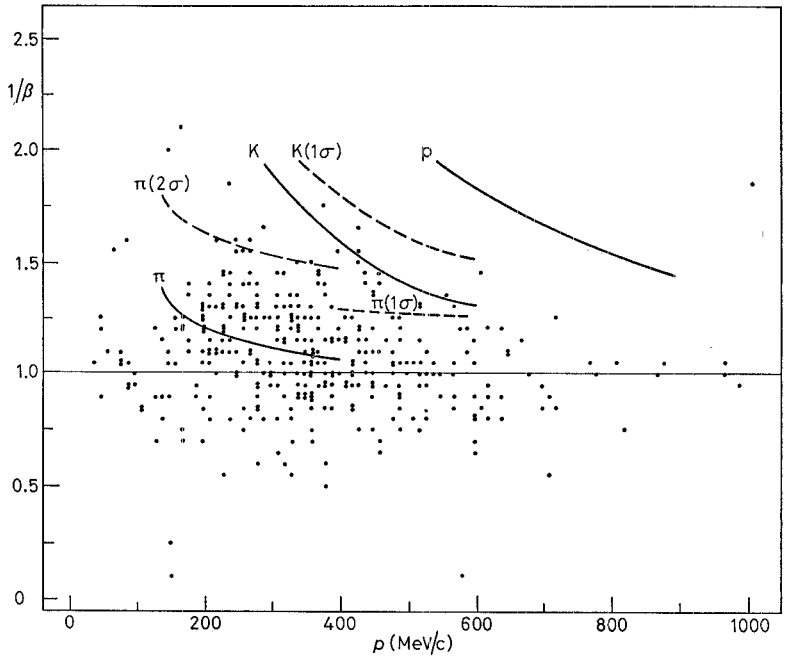

Fig. 3. – Scatter plot of $1/\beta$ *vs.* p for negative particles which satisfy the selection criteria. Full lines and dashed lines are the same as in the previous figure.

The scatter plot of $1/\beta$ *vs.* p is shown in fig. 2 for all the tracks which satisfy the *a*), *b*) and *c*) conditions. The presence of a small contamination ($\sim$ 5%) of protons, coming from the beam gas background interactions, is clearly visible. Obviously no such contamination is present in the corresponding scatter plot for negative particles (fig. 3). In the figures the curves corresponding to proton, kaon and pion masses are reported together with those obtained by adding one or two standard deviations to the time-of-flight measurement.

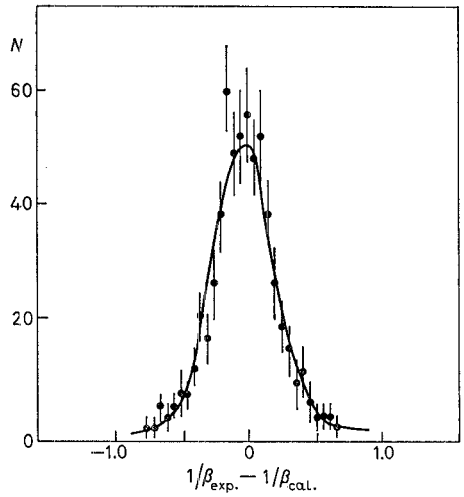

Fig. 4. – Time-of-flight resolution for particles with momentum less than 600 MeV/c. β_{cal} is the value obtained from the momentum measurement under the hypothesis of pion production. Full line is the fitted Gaussian with $\sigma = 0.22$, which means $\sigma_t = 0.73$ ns in time of flight.

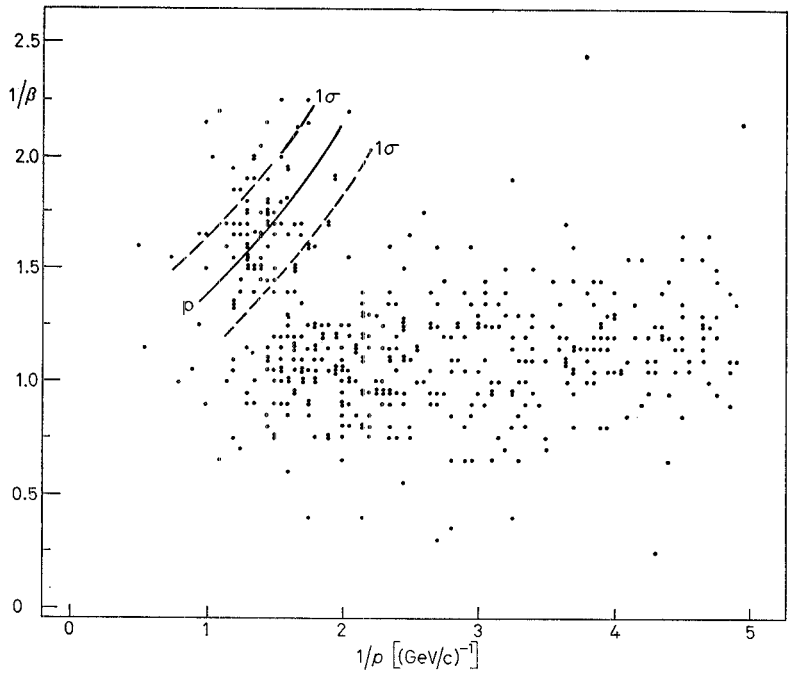

Fig. 5. – Scatter plot of $1/\beta$ *vs.* $1/p$ for positively charged particles, including also events which do not satisfy the acoplanarity condition $\Delta\varphi \geqslant 10°$; protons due to beam gas background are well centred around the curve $1/\beta = \sqrt{1 + m_p^2/p^2}$; dashed lines represent the same curve displaced by one standard deviation in time of flight.

The time-of-flight resolution is obtained from fig. 4, where the distribution of $1/\beta_{\text{exper}} - 1/\beta_{\text{calc}}$ for tracks with momentum less than 600 MeV/c is reported. The cut has been chosen in order not to have the proton contamination; β_{calc} is the value obtained from the measured value of the momentum of the track by assuming the particle to be a pion. The distribution obtained is well fitted by a Gaussian function with zero mean value and standard deviation $\sigma = 0.22$. The corresponding time-of-flight resolution $\sigma_t = 0.22 \times 3.3 = 0.73$ ns gives a standard deviation of 0.51 ns for the single counter. The correction to the time-of-flight measurement, used in order to take the pulse

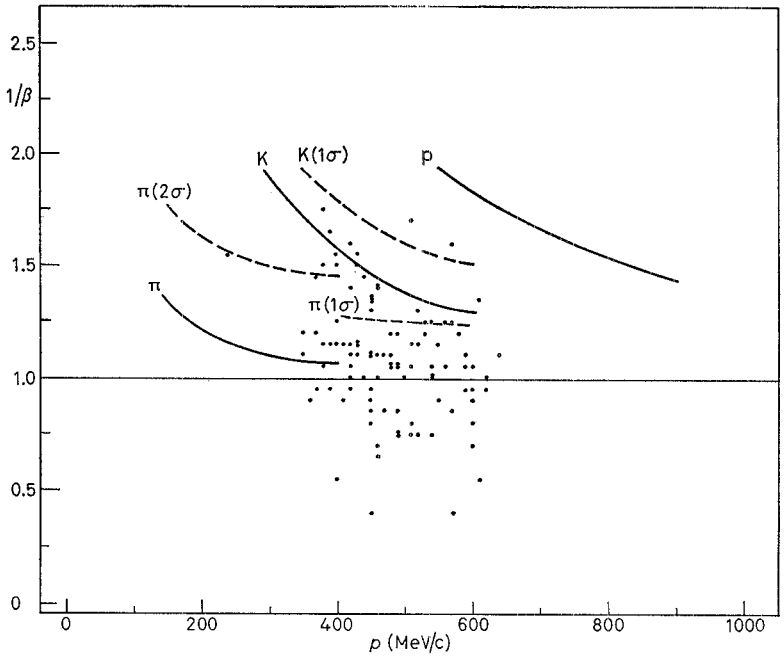

Fig. 6. – Scatter plot of $1/\beta$ *vs.* p for all selected particles, both positive and negative particles having range R not greater than the kaon range increased by 30 g/cm² ($R \leqslant R_K + 30$ g/cm²).

height A of the counters into account, is of the type $K/\sqrt{A}$ [2]; the constant K has been obtained, for each counter, by optimizing the time-of-flight spectrum given by cosmic rays. In order to check this correction, the scatter plot of $1/\beta$ *vs.* $1/p$ for the positively charged tracks is reported in fig. 5, where events

(2) W. BRAUNSCHWEIG, E. KÖNIGS, W. STRUM and W. WALLRAFF: *Nucl. Instrum. Methods*, **134**, 261 (1976).

which do not satisfy the acoplanarity condition $\Delta\varphi \geqslant 10°$ are also included. The points around the region corresponding to the proton mass are well centred with respect to the curve $1/\beta = \sqrt{1 + m_p^2/p^2}$, which indicates that the pulse height correction works well.

It is not possible to recognize singly the K-mesons present in the sample because of the resolution obtained in $1/\beta$ and because the fraction of tracks which could be ascribed to kaons is rather small, as can be seen from fig. 3 by assuming all the points lying above the kaon mass curve be kaons. For this purpose we used also the range measurement which can be based on the information coming from S_3, S_4 (S_3', S_4') and from the thick-plate spark chambers outside the coil. The scatter plot of $1/\beta$ *vs.* p for all the tracks having range R not greater than the corresponding kaon range, increased by 30 g/cm² ($R \leqslant R_K + 30$ g/cm²), is given in fig. 6. The corresponding scatter plot for only the negative particles is reported in fig. 7.

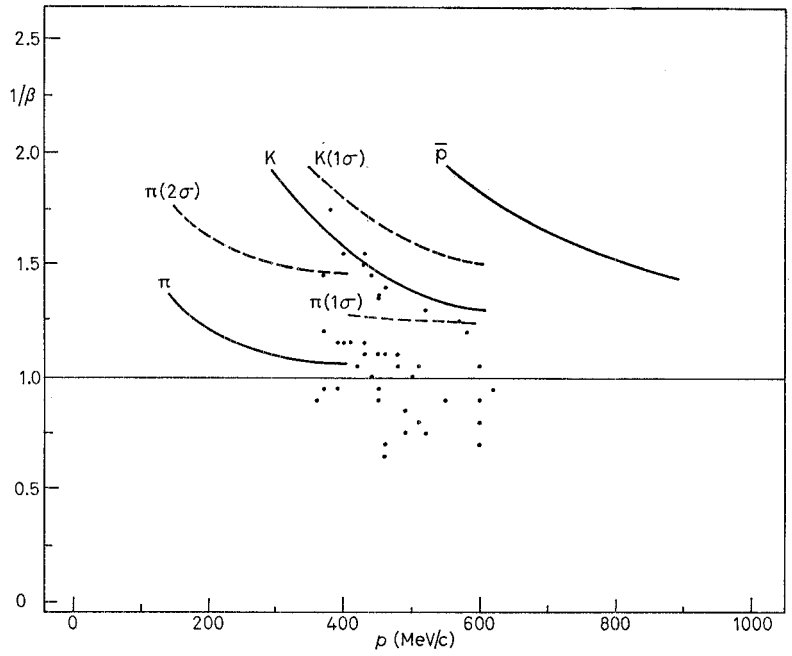

Fig. 7. – Scatter plot of $1/\beta$ *vs.* p for negative particles having range R not greater than the kaon range increased by 30 g/cm² ($R \leqslant R_K + 30$ g/cm²).

On the basis of the scatter plot reported in fig. 6, the number of tracks which can be identified as kaons can be estimated. The events have been divided in three energy intervals ($\sqrt{s} = (1.4 \div 1.6)$, $(1.75 \div 1.95)$, $(2.1 \div 2.3)$ GeV) and in two momentum intervals of the kaons ($(400 \div 500)$, $(500 \div 600)$ MeV/c)

TABLE I. – *Kaon fractions.* N_1 = number of selected tracks, N_2 = number of selected tracks with $R \leqslant R_K + 30\,g/cm^2$, N_3 = number of selected tracks with $R \leqslant R_K + 30\,g/cm^2$ and with $1/\beta \geqslant 1/\beta_\pi + 1$ standard deviation, B = background of pions expected on N_3, calculated from $1/\beta$ distribution; $\varepsilon = \varepsilon_p \cdot \varepsilon_D \cdot \varepsilon_R \cdot \varepsilon_\beta = 0.58$ for $400 \leqslant p \leqslant 500$ MeV/c and $= 0.46$ for $500 \leqslant p \leqslant 600$ MeV/c, where ε_p is the efficiency for momentum cut, ε_D for K decay, ε_β for $1/\beta$ cut and ε_R is the efficiency on range measurement.

$\sqrt{s}$ (GeV)	p (MeV/c)	N_1	N_2	N_3	B	$K/\text{tot} = (N_3 - B)/(N_1 \cdot \varepsilon)$
1.4 ÷1.6	400÷500	52	20	5	2.6	0.08 ± 0.07
	500÷600	22	13	2	2.2	-0.02 ± 0.12
1.75÷1.95	400÷500	71	26	10	2.8	0.18 ± 0.07
	500÷600	39	17	3	2.4	0.03 ± 0.08
2.1 ÷2.3	400÷500	17	7	3	0.7	0.23 ± 0.15
	500÷600	6	5	1	0.9	0.04 ± 0.22

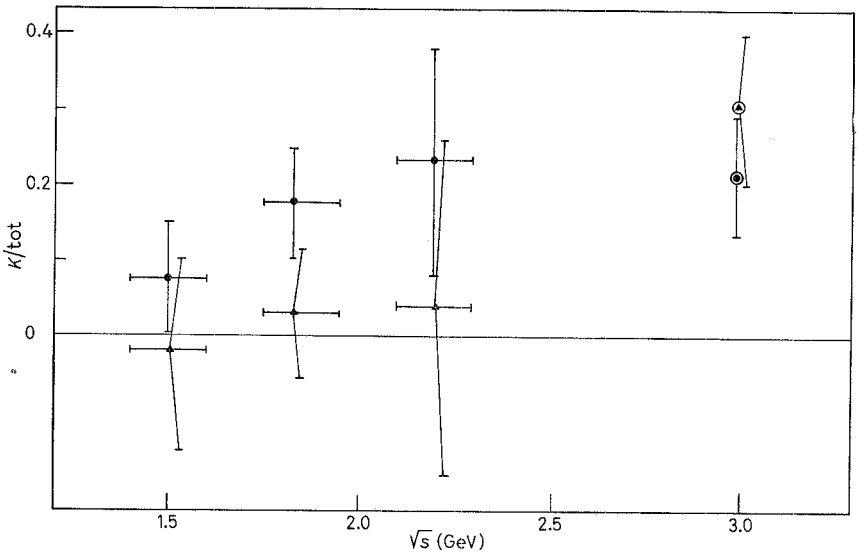

Fig. 8. – Ratio of tracks which can be identified as kaons on the basis of momentum and time of flight measured, over total number of selected tracks, as a function of the c.m. energy: • $400 \leqslant p \leqslant 500$ MeV/c and ▲ $500 \leqslant p \leqslant 600$ MeV/c; points at $\sqrt{s} = 3.0$ GeV are SLAC-LBL data [3].

[3] B. RICHTER: *Proceedings of the XVII International Conference on High-Energy Physics* (London, 1974), p. IV-37.

In table I the data are reported in detail together with the results obtained. The results are also reported in fig. 8.

It is also possible to evaluate the ratio of kaons with momentum between 200 and 400 MeV/c which, therefore, stop in the coil; for those tracks the time of flight has been triggered by the decay products of the K^+ or by the secondaries produced in the end range interaction of the K^-.

A Monte Carlo calculation gives for the detection efficiency of the decay products of the K^+ which stop in the coil a mean value of 0.3 for $200 \leqslant p_K \leqslant 400$ MeV/c, while the detection efficiency of the secondaries of the K^- interaction in the same momentum range turns out to be $\varepsilon_d \simeq 0.1$. In fig. 9 the ratio K/total *vs.* $\sqrt{s}$ is shown for this momentum interval.

Due to the lack of statistics it is not meaningful to subdivide the data into more bins both as a function of the momentum and of the c.m. energy.

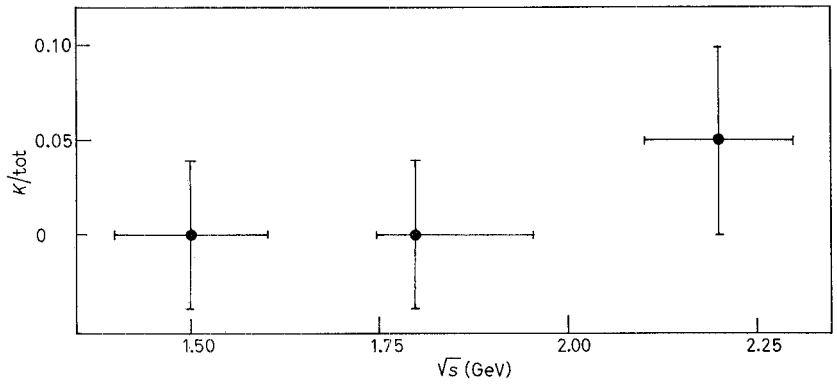

Fig. 9. – Ratio of tracks which can be identified as kaons in the momentum range $200 \leqslant p \leqslant 400$ MeV/c over the total number of selected tracks.

3. – Inclusive distributions.

The inclusive momentum distribution has been obtained directly from the momenta of all the particles of the selected and measured events. The momentum resolution of the whole system determined from the μ-pair events is $\sigma_p/p = 0.078$ at $p = 780$ MeV/c. In fig. 10 the invariant cross-section $E\,\mathrm{d}^3\sigma/\mathrm{d}p^3$ is reported in arbitrary units as a function of the energy E of the single particle which is supposed to be a pion; the momentum cut of the apparatus is 80 MeV/c. All the tracks of the events in the energy range $1.4 \leqslant \sqrt{s} \leqslant 2.3$ GeV are reported excluding those with $p < 160$ MeV/c and probability less than 5% to be pions on the basis of the analysis explained in the previous section in order to minimize the contamination due to low-momentum electrons. Also the events with an identified proton have not

been considered. The data are consistent with a distribution of the type

$$E\,\frac{\mathrm{d}^3\sigma}{\mathrm{d}p^3} = B\exp\left[-E/kT\right],$$

where $kT = (145 \pm 3)$ MeV ($\chi^2/\mathrm{DF} = 69/62$).

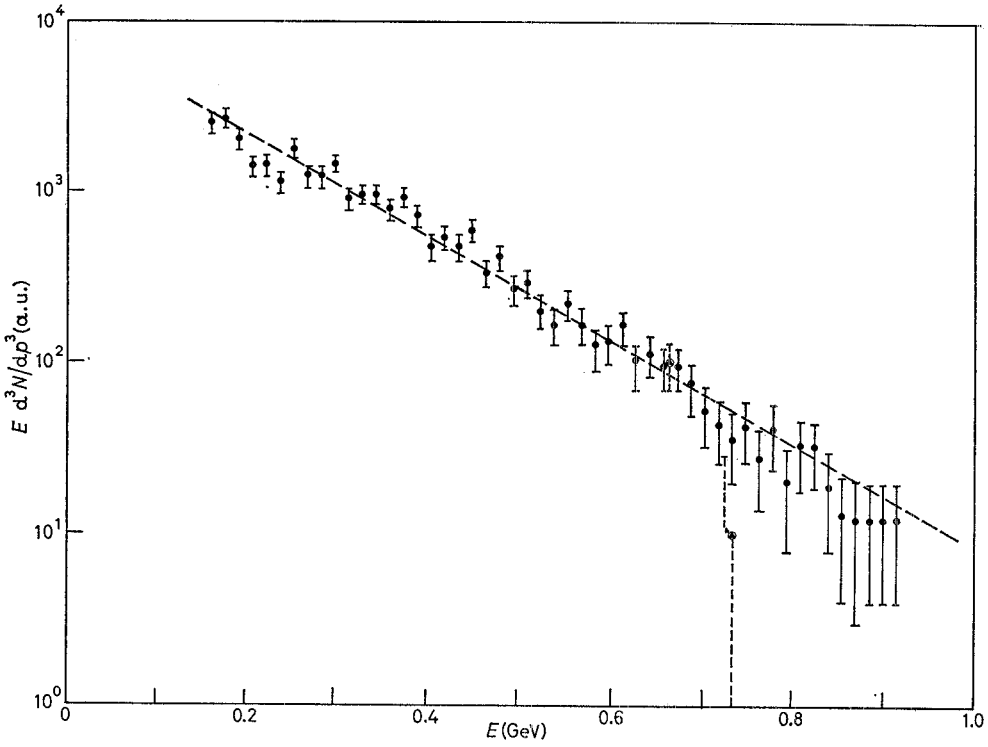

Fig. 10. – Inclusive momentum distribution of particles produced in the c.m. energy range $1.4 \leqslant \sqrt{s} \leqslant 2.3$ GeV as a function of the energy of the particle for pions (•) and kaons (▲). The dashed line is the exponential fit of the data.

In the same figure the data relative to the tracks identified as kaons have been plotted; these points fit quite well the pion curve. Dividing the data into 3 energy regions and calculating the corresponding fits, we obtain

I) $\sqrt{s} = (1.4 \div 1.6)$ GeV, $kT = (149 \pm 7)$ MeV, $\chi^2/\mathrm{DF} = 54/41$,

II) $\sqrt{s} = (1.75 \div 1.95)$ GeV, $kT = (151 \pm 5)$ MeV, $\chi^2/\mathrm{DF} = 47/54$,

III) $\sqrt{s} = (2.10 \div 2.30)$ GeV, $kT = (133 \pm 8)$ MeV, $\chi^2/\mathrm{DF} = 45/54$

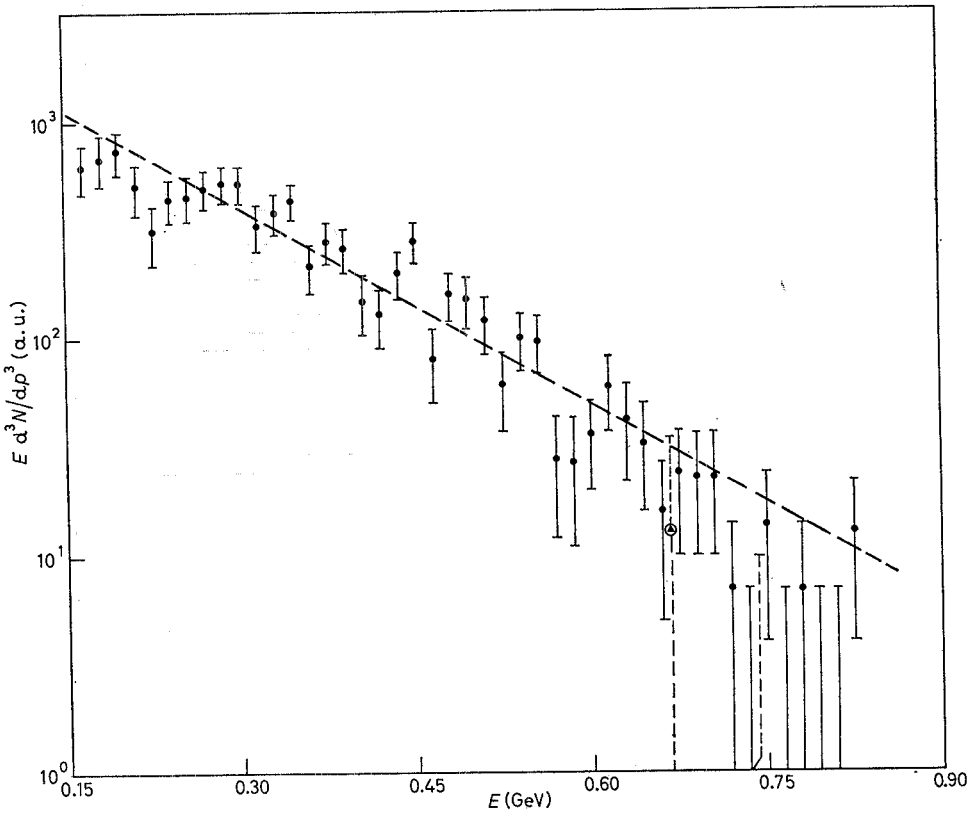

Fig. 11. – Inclusive momentum distribution of particles produced in the c.m. energy range $1.4 \leqslant \sqrt{s} \leqslant 1.6$ GeV as a function of the energy of the particle for pions (•) and kaons (▲). The dashed line is the exponential fit of the data.

(see fig. 11, 12, 13). The points belonging to the kaons agree quite well at the different energies to the pion data. A Monte Carlo calculation shows that the momentum resolution does not affect appreciably the kT values obtained.

For the three energy intervals, the mean energy of the particle is, respectively,

I) $\langle E_\pi \rangle = (358 \pm 7)$ MeV,

II) $\langle E_\pi \rangle = (373 \pm 7)$ MeV,

III) $\langle E_\pi \rangle = (365 \pm 12)$ MeV,

and as a consequence the mean multiplicity is

I) $\langle n \rangle = \sqrt{s}/\langle E_\pi \rangle = 4.2 \pm 0.1$,

II) $\langle n \rangle = \sqrt{s}/\langle E_\pi \rangle = 4.9 \pm 0.1$,

III) $\langle n \rangle = \sqrt{s}/\langle E_\pi \rangle = 6.0 \pm 0.2$.

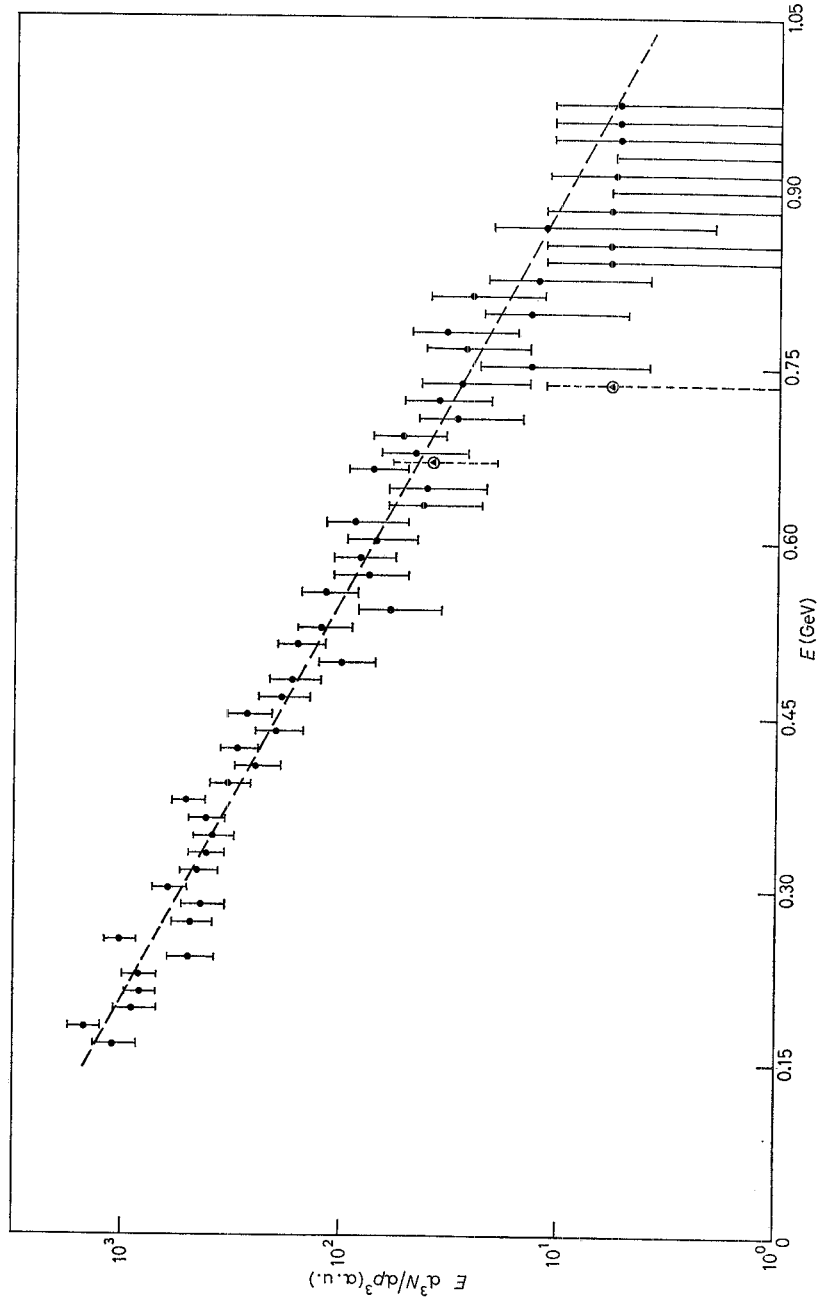

Fig. 12. – Inclusive momentum distribution of particles produced in the c.m. energy range $1.75 \leqslant \sqrt{s} \leqslant 1.95$ GeV as a function of the energy of the particle for pions (•) and kaons (▲). The dashed line is the exponential fit of the data.

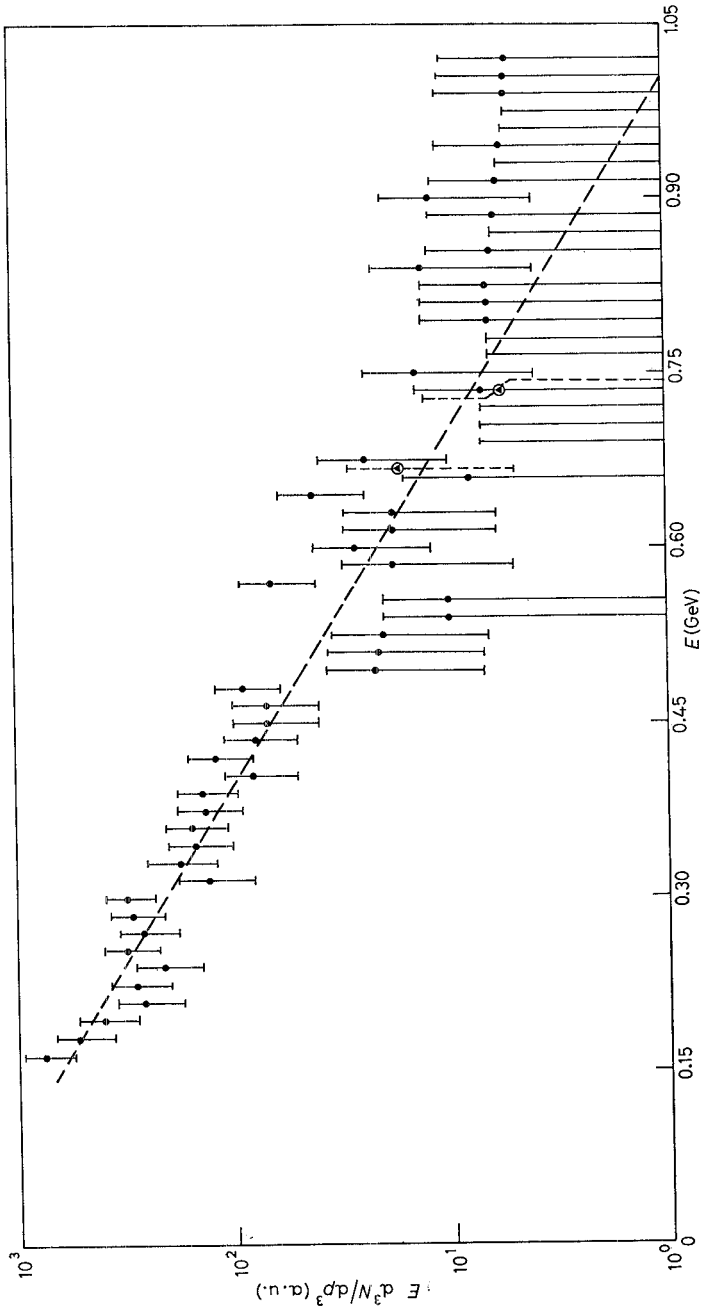

Fig. 13. – Inclusive momentum distribution of particles produced in the c.m. energy range $2.10 \leqslant \sqrt{s} \leqslant 2.30$ GeV as a function of the energy of the particle for pions (•) and kaons (▲). The dashed line is the exponential fit of the data.

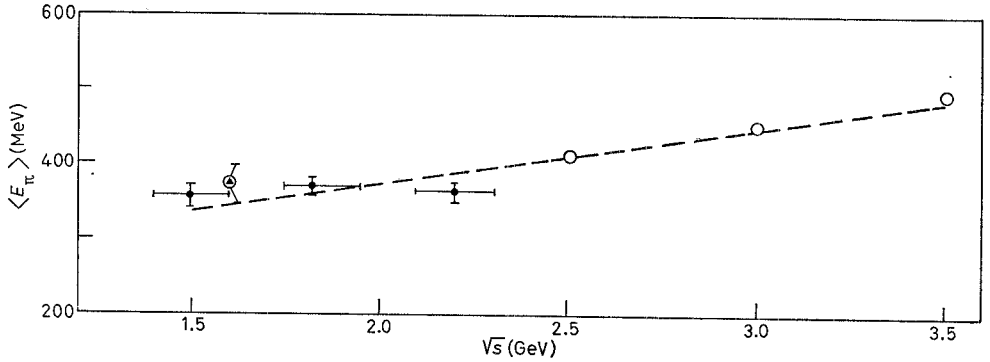

Fig. 14. – Mean value of the energy of the selected tracks under the hypothesis of pure pion production as a function of the c.m. energy: • are the new data, ▲ is a previous MEA value (4) and o are SPEAR data (5). The dashed line is the prediction of the covariant statistical model (6) normalized to the 2.5 GeV value.

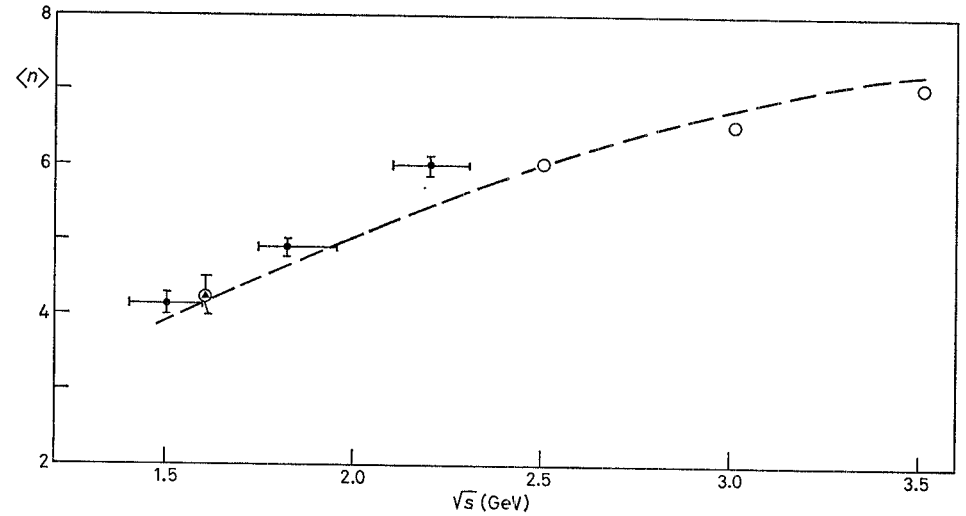

Fig. 15. – Mean multiplicity of the events as a function of the c.m. energy: • are the new data, ▲ is a previous MEA value and o are the SPEAR data. The dashed line is the prediction of the covariant statistical model normalized to the 2.5 GeV value.

(4) B. ESPOSITO, F. FELICETTI, A. MARINI, I. PERUZZI, M. PICCOLO, F. RONGA, A. NIGRO, D. BISELLO, M. NIGRO, L. PESCARA, P. SARTORI, R. BERNABEI, S. D'ANGELO, P. MONACELLI, L. PAOLUZI, G. PIANO MORTARI, A. SCIUBBA and F. SEBASTIANI: *Lett. Nuovo Cimento*, **19**, 21 (1977).

(5) R. SCHWITTERS: *Proceedings of the International Symposium on Lepton and Photon Interactions at High Energies* (Stanford, Cal., 1975), p. 5.

(6) J. ENGELS, K. SHILLING and H. SATZ: *Nuovo Cimento A*, **17**, 535 (1973).

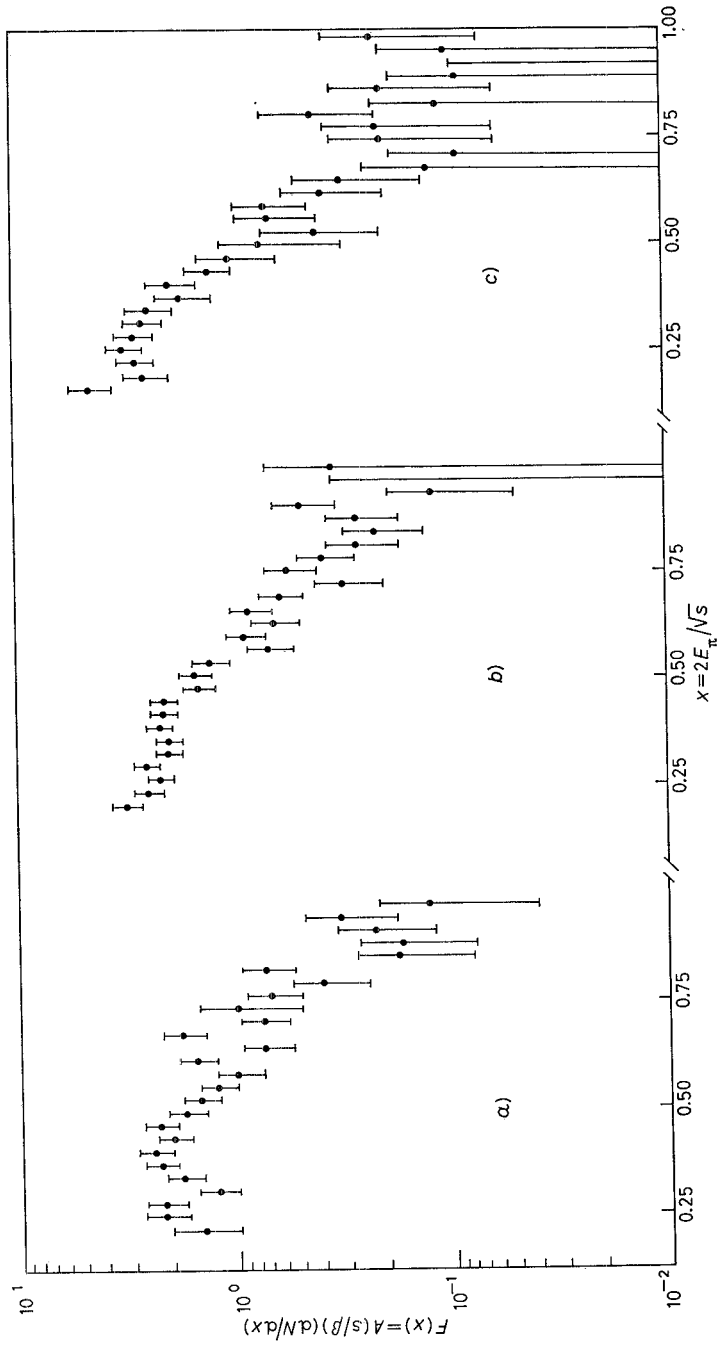

Fig. 16. – $F(x)$ distributions (see the text) for *a*) $1.4 \leqslant \sqrt{s} \leqslant 1.6$ GeV, *b*) $1.75 \leqslant \sqrt{s} \leqslant 1.95$ GeV, *c*) $2.10 \leqslant \sqrt{s} \leqslant 2.30$ GeV.

The energy cut introduced by the apparatus has been taken into account in the calculation of the mean energy by extrapolating the experimental behaviour by means of the corresponding $B \exp[-E/kT]$ function; this correction is rather low (~ 10 MeV). The values obtained for $\langle E_\pi \rangle$ and $\langle n \rangle$ are reported in fig. 14, 15 together with those obtained at SPEAR ([3]) and with the covariant statistical model ([4]) normalized to the experimental value at 2.5 GeV. The values of $\langle E_\pi \rangle$ and $\langle n \rangle$ are affected by an uncertainty less than or equal to $\pm 10\%$, due to the different values of the efficiencies of the trigger for the various final-state configurations and to the energy dependence of these efficiencies; the errors reported are only statistical.

Figure 16 shows the normalized distributions $F(x) = (As/\beta)(\mathrm{d}N/\mathrm{d}x)$, where the constant A has been chosen so that $\int_0^1 F(x)\,\mathrm{d}x = 1$. The relative increase with $\sqrt{s}$ of the low-x part of the distributions is due to the increasing multiplicity.

● RIASSUNTO

Si riportano i risultati di uno studio inclusivo sulla produzione di particelle cariche prodotte nella reazione e^+e^- → molti adroni nell'intervallo di energia del centro di massa $\sqrt{s} = (1.4 \div 2.3)$ GeV. È stato misurato il rapporto tra il numero di $K^\pm$ rivelato dall'apparato MEA ed il corrispondente numero totale di particelle cariche. Si presentano le distribuzioni inclusive dei momenti delle particelle cariche rivelate per tre intervalli di $\sqrt{s}$ ed inoltre — in funzione di $\sqrt{s}$ — l'energia media e la molteplicità media delle particelle cariche rivelate.

Резюме не получено.

B. ESPOSITO, *et al.*
21 Febbraio 1980
Il Nuovo Cimento
Serie 11, Vol. **55** A, pag. 437-452